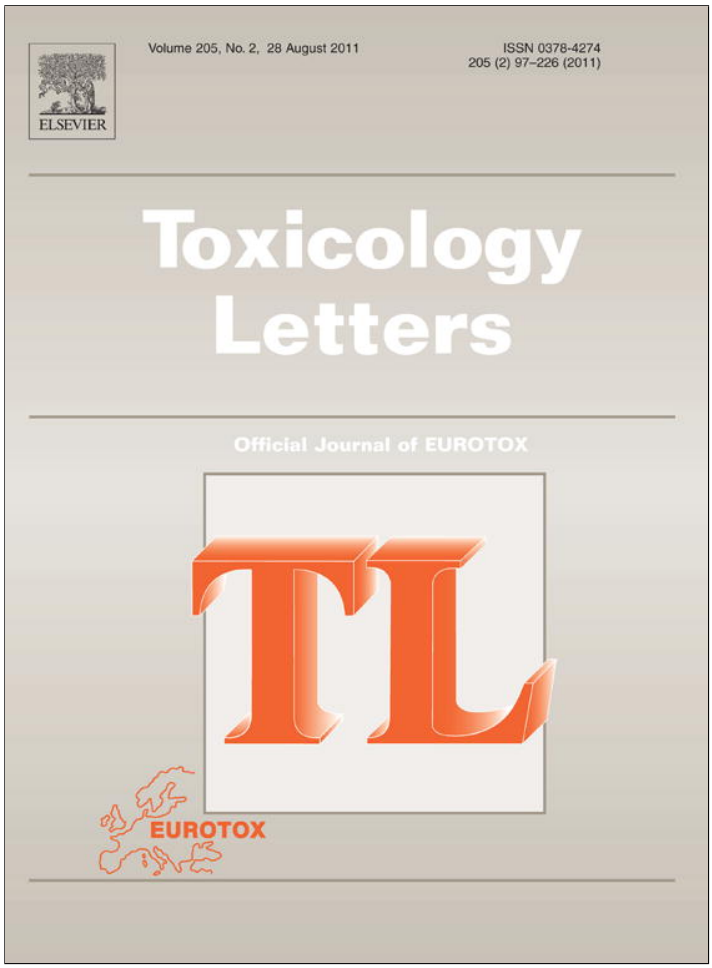

Toxicology Letters 205 (2011) 173–182

Contents lists available at ScienceDirect

Toxicology Letters

journal homepage: www.elsevier.com/locate/toxlet

EGCG-meditated cyto- and genotoxicity in HaCat keratinocytes is impaired by cell-mediated clearance of auto-oxidation-derived H_2O_2: An algorithm for experimental setting correction

Leonilla Elbling[a,*], Irene Herbacek[a], Rosa-Maria Weiss[a], Christopher Gerner[a], Petra Heffeter[a], Christian Jantschitsch[b], Franz Trautinger[c], Michael Grusch[a], Heinrich Pangratz[d], Walter Berger[a,*]

[a] Department of Medicine I, Institute of Cancer Research, Medical University Vienna, Borschkegasse 8a, 1090 Vienna, Austria
[b] University Kiel, Department of Dermatology, Germany
[c] Karl Landsteiner Institute for Dermatological Research, St. Poelten, Austria
[d] Technical University of Vienna, Austria

ARTICLE INFO

Article history:
Received 17 March 2011
Received in revised form 1 June 2011
Accepted 4 June 2011
Available online 15 June 2011

Keywords:
Cell number/volume ratio
Epigallocatechin-3-gallate
Hydrogen peroxide
Free radicals
Polyphenolic compounds

ABSTRACT

Several lines of evidence suggest that besides antioxidant also prooxidant properties are crucially involved in cytotoxic and protective activities of the major green tea catechin epigallocatechin-3-gallate (EGCG) *in vitro* (Elbling et al., 2011). Furthermore recent data suggest that EGCG induces oxidative stress also *in vivo* (Li et al., 2010). Here we set out to identify factors modulating cellular effects of EGCG *in vitro*. Using the HaCat keratinocytes model, we demonstrate that the cytotoxic, genotoxic and signal-activating effects of EGCG are significantly dependent on the ratio of cell number to working volume. Treatment with identical EGCG concentrations at altered experimental settings resulted in IC_{50} values differing up to orders of magnitude and could even exert contradictory effects. This effect was based on cell-mediated clearance of autooxidation-derived H_2O_2 from the supernatant. In order to estimate EGCG/H_2O_2 concentrations equally effective under different settings, we have rationally derived and experimentally verified a simple algorithm relating concentration, working volume, cell number and – indirectly – exposure time. Algorithm application resulted in similar H_2O_2 clearance curves from cell supernatants as well as comparable EGCG/H_2O_2 effects at different settings. Our results demonstrate the importance of standardized experimental settings when investigating cytotoxic and/or beneficial effects of autooxidizing compounds.

1. Introduction

Plant polyphenols, like the green tea epigallocatechin-3-gallate (EGCG), are in the focus of interest as agents with potentially antioxidant and health beneficial properties (Halliwell, 2008; Higdon and Frei, 2003; Lambert et al., 2007a; Yang et al., 2009a). The list includes several medical conditions including rheumatoid arthritis, high cholesterol levels, impaired immune function, cardiovascular disease and cancer with reactive oxygen species (ROS) suggested as causal relationship (Khan and Mukhtar, 2007; Yang et al., 2007, 2009b). Furthermore antiviral (Song et al., 2005) and bactericidal activities (Ikigai et al., 1993) but also photoprotection from UV light (Afaq et al., 2003; Elmets et al., 2001) have been attributed to EGCG. The most prominent mechanisms of EGCG proposed to be causative for several beneficial effects include reduction of cellular damage due to anti-oxidant and reactive oxygen as well as nitrogen species-scavenging activities (Anderson et al., 2001; Halliwell, 2008; Higdon and Frei, 2003; Hou et al., 2004; Sang et al., 2005; Yang et al., 2002). However, also inhibitory effects on signal transduction pathways resulting in cell cycle arrest and/or cell death have been described (Ahmad et al., 2000; Hou et al., 2004; Khan et al., 2006; Yang et al., 2006). Moreover, EGCG-induces activation of MAP kinases (Yu et al., 2000) and the downstream redox-sensitive Keap1–Nrf2–ARE signalling pathway (Na et al., 2008) regulating phase II detoxifying and antioxidant enzymes (Na et al., 2008; Nguyen et al., 2009). These data indicate that the antioxidant effects of EGCG might be related to prooxidant activities.

The issue whether plant polyphenols autooxidation is a mere *in vitro* artefact or also an *in vivo* phenomenon has been extensively and controversially discussed in the literature (Gutteridge and Halliwell, 2010; Halliwell, 2008; Lambert et al., 2007b; Long

Abbreviations: CN, cell number; CVI, cell number volume index; DCFH-DA, 2′,7′-dichlorodihydrofluorescein diacetate; EGCG, epigallocatechin-3-gallate; JC-1, 5,5′,6,6′-tetrachloro-1,1′,3,3′-tetraethyl-benzimidazolylcarbocyanine iodine; MTT, 3-(4,5-dimethylthiazol-2-yl)-2,5-diphenyltetrazolium bromide; ROS, reactive oxygen species; TB, trypan blue.

* Corresponding authors. Fax: +43 1 4277 65169.
E-mail addresses: leonilla.elbling@meduniwien.ac.at (L. Elbling), walter.berger@meduniwien.ac.at (W. Berger).

0378-4274/$ – see front matter © 2011 Elsevier Ireland Ltd. All rights reserved.
doi:10.1016/j.toxlet.2011.06.001

et al., 2007; Yang et al., 2009b). Recently this topic has received new significance by the observation of oxidative cellular damages in human lung cancer xenograft tumors after EGCG treatment (Li et al., 2010). This demonstration of prooxidative activities of EGCG *in vivo* together with the significant role of EGCG-generated H_2O_2 in cellular protection against oxidative stress *in vitro* (Elbling et al., 2011) suggest autooxidation as an important component of EGCG-mediated activities.

Earlier studies have shown that H_2O_2-mediated cytotoxicity exerts cell density dependence predominantly as a phenomenon of exponential growth as compared to confluence (Bello et al., 2003; Long et al., 2003; Spitz et al., 1987). Characteristically exogenously added H_2O_2 as well as H_2O_2 formed within aqueous EGCG solutions is cleared from media that contain cells (Elbling et al., 2005, 2011; Hong et al., 2002). The present study was undertaken to examine, whether prooxidant activities of EGCG are influenced by changes in the experimental condition regarding the ratio of cell number and working volume or – in other words – EGCG amount per cell. To avoid the impact of contact inhibition at cell confluence, all experiments were performed in proliferating cell cultures. Using HaCat keratinocytes (Boukamp et al., 1988) at different subconfluent settings, we demonstrate in the present study that the ratio between cell number and working volume has pronounced effects on (1) H_2O_2 clearance, (2) overall cellular oxidative stress and (3) cyto(geno)toxic cell damaging and signal transducing effectiveness of EGCG as compared to pure H_2O_2. Consequently, we have developed an algorithm allowing to estimate equally effective EGCG/H_2O_2 concentrations in proliferating HaCat cells under different experimental conditions needed in diverse cell biological assays.

2. Materials and methods

2.1. Reagents

Reagents were from Sigma–Aldrich, except EGCG (99.7% purity, Alexis Corp.), trypan blue (TB), JC-1 and 2′,7′-dichlorodihydrofluorescein diacetate (DCFH-DA) from Fluka and agarose from Invitrogen. Solutions including the EGCG stock (10 mM in 4 °C PBS) were freshly prepared except DCFH-DA (33.4 mM stock in DMSO; Liquid, Hybri-Max, minimum 99.7%) stored at −80 °C.

2.2. Cells and treatment

Immortalized keratinocytes (HaCat) (Boukamp et al., 1988) were maintained in RPMI-1640 (Invitrogen) supplemented with 10% heat-inactivated foetal calf serum (FCS; PAA, Traun, Austria) at 37 °C in a humidified 5% CO_2 atmosphere. Cells were treated 24 h after seeding (the reference setting was defined as 7×10^5 cells/2 ml/well of a 6-well plate) in complete medium. At this time point the cell number roughly corresponded to the original seeding cell number and confluence was below 60%. Different modifications of the experimental conditions regarding the relationship of cell number to working volume (but at stable drug concentrations) were performed. EGCG and H_2O_2 were used as ready prepared solutions used immediately after solubilisation in complete medium preconditioned in the incubator for 24 h in order to keep experimental derived stress as low as possible. All experiments were set up in duplicate (6-well plate) or triplicate (96-well plate) and performed at least 3 times.

2.3. Trypan blue assay

Cells were trypan blue stained (detached plus attached cells) for determining viability and cell death.

2.4. JC1 staining

Cells were JC-1 stained according to the manufacturer's instructions (Mitochondria staining Kit, Sigma–Aldrich) and analysed by flow cytometry (FACSCalibur™, BD Systems). JC1 is a cationic dye to indicate depolarization of the mitochondrial membrane potential as an early step of apoptosis activation by the endogenous pathway (Heffeter et al., 2006). JC-1 forms red-fluorescent aggregates within the mitochondria of undamaged cells while it remains as green-fluorescent monomer in the cytosol of apoptotic/necrotic cells.

2.5. Clonogenic survival assay

Cells at 1×10^3 cells/2 ml were treated in 6-well plates. Crystal violet (0.5%) staining of methanol (−20 °C) fixed cells was done after additional 10 days in culture. Survival curves were generated after dye solubilisation with Sorenson's solution. Absorbance at 595 nm represents the relative clonogenic survival.

2.6. SCGE assays (comet assays)

Cells were processed for comet assays (Tice et al., 2000) performed as published (Elbling et al., 2005). Coded slides were examined with a fluorescence microscope (NIKON Eclipse E600) equipped with an automated digital imaging system (COMET Assay IV, Perceptive Instruments, UK). Data expressed as % tail DNA (Burlinson et al., 2007) were collected from 150 cells per experiment in triplicate (50 cells/slide/culture). Data are shown as box plots where the bottom and top of the box represent the 25th and 75th percentile and the band near the middle of the box the median. Upper and lower whiskers show maximum and minimum values. All experiments were independently repeated at least twice. The extent of DNA migration is indicative for DNA damage.

2.7. Detection of intracellular ROS (DCFH-DA assay)

Measurement of the overall cellular oxidative stress after EGCG and H_2O_2 treatment was performed using the cell-permeable and ROS-sensitive probe DCFH-DA (Wang and Joseph, 1999), which generates the fluorescent 2′,7′-dichlorofluorescein (DCF) upon enzymatic reduction and subsequent oxidization by various ROS (Royall and Ischiropoulos, 1993). Cells labeled with DCFH-DA followed by treatment were forwarded to analysis by flow cytometry as published (Elbling et al., 2005). Data are derived from at least three independent experiments.

2.8. Measurement of H_2O_2 (FOX-assay)

Cells were treated with EGCG or H_2O_2 and the content of H_2O_2 was determined by the ferrous ion oxidation-xylenol orange method (FOX)-assay following the aqueous-compatible version FOX-1 using the PeroXOquant™ Quantitative Peroxide Assay Kit (PIERCE Biotechnology) according to the manufacturer's protocol. H_2O_2 specificity was confirmed by the abrogation of colour formation in the presence of catalase (100 U/ml) (Wolff, 1994). Data are derived from at least three independent experiments.

2.9. Immunoblotting

Total cell extracts were prepared after different time intervals of treatment and used for Western blotting as described previously (Elbling et al., 2005) to assess phosphorylated ERK1/2 (pERK44/42, clone 20G11, dilution 1:1000) and total ERK1/2 (polyclonal Ab #9102, dilution 1:2000) (Cell Signalling Technology). Visualization of signals was performed with goat anti-rabbit secondary antibody (dilution 1:10000) (Santa Cruz Biotechnology) and Chemi-smart 5100 chemiluminescence detection system (Vilber Lourmat). Exposure times were adapted to avoid any saturation of the signals.

2.10. Statistical analyses

Comet assay results are not normally distributed. Therefore, as suggested by Collins (2004), Tice et al. (2000), we used the non-parametric Mann–Whitney *U* test and Kruskal–Wallis test that calculate differences between 2 and more than 2 unpaired groups, respectively. All other comparisons for differences among two and more than two data sets (means ± SD) were performed by applying Student's *t*-test and ANOVA with Bonferroni test, respectively. Statistical analyses were performed using GraphPad Prism version 4.02 for Windows, GraphPad Software (San Diego, California, USA). Significance was established at values of $p < 0.05$.

3. Results

3.1. Reduction of the ratio between cell number and working volume enhances cyto- and genotoxic effects of EGCG and H_2O_2

In a first step, the cytotoxic and genotoxic activities of defined EGCG and H_2O_2 concentrations were determined at three different conditions regarding the ratio of cell number/working volume. The initial reference condition was 7×10^5 cells/2 ml/well of a 6-well plate compared to reduced cell numbers of 3.5×10^5/2 ml (50%) and 1.75×10^5/2 ml (25%). Drug-free control groups with these settings did not show any differences in mitochondrial function as measured by JC-1 staining (Fig. 1A), cell growth (Fig. 1B) and DNA damage determined by comet assays (Fig. 1D, one representative value of untreated cells). However, equal EGCG and

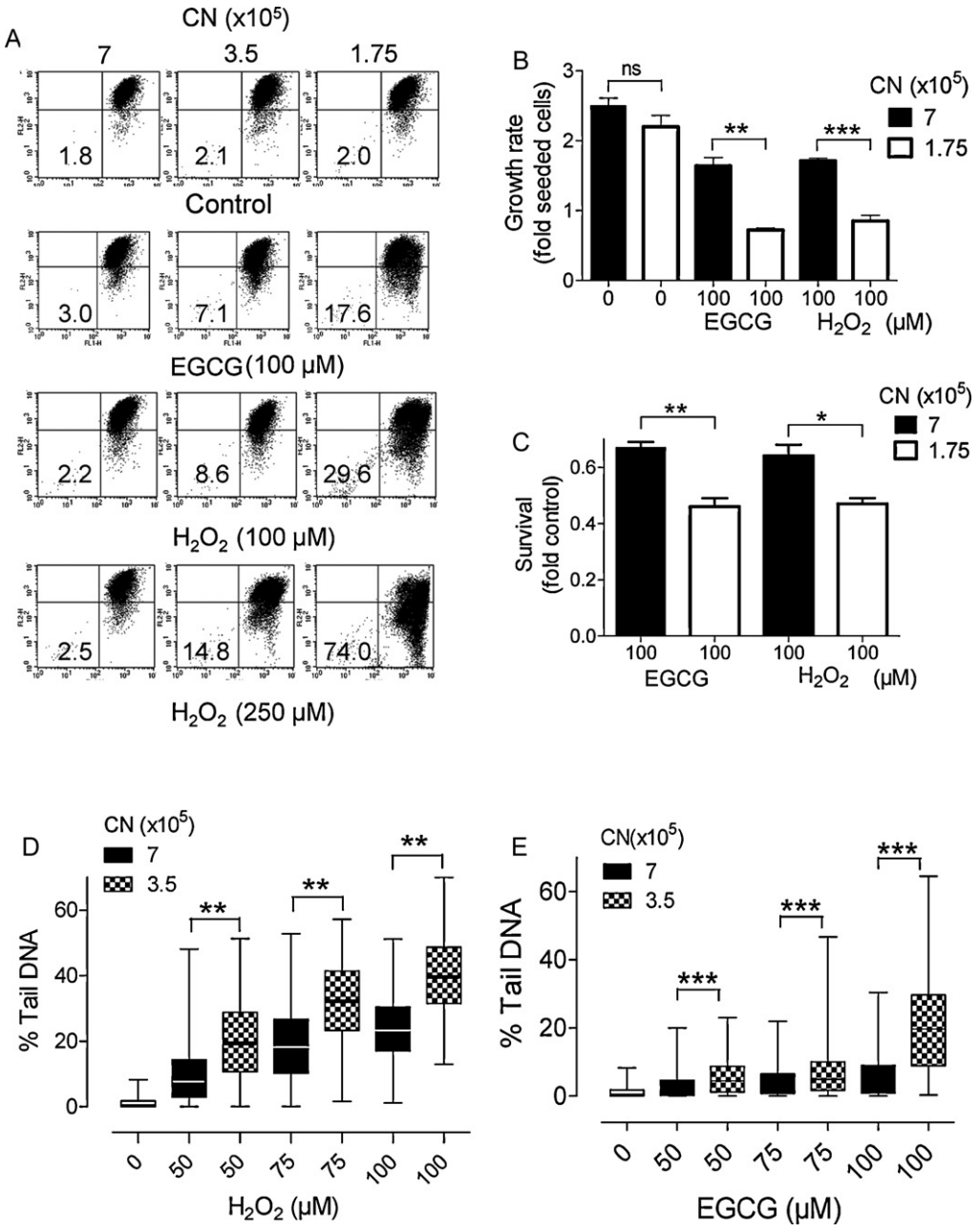

Fig. 1. Changes in cell number/working volume settings affect EGCG- and H_2O_2-induced cyto- and genotoxicity. Cell numbers (CNs) ($\times 10^5$) were changed as indicated and all working volumes were maintained at 2 ml. (A) Mitochondrial membrane potential ($\Delta\Psi_m$) was determined by JC-1 staining after 4 h treatment. FACS plots of FL-1 (green emission of monomeric JC-1) versus FL-2 (orange emission of JC-1 aggregates) are presented. Inserted numbers indicate percentages of cells characterised by reduced membrane potential and located in the lower right quadrant (green fluorescence). Three independent experiments delivered comparable results. (B) Growth rate (cell count 48 h after seeding including 24 h treatment) was determined by the trypan blue method (data are means ± SD; $n = 6$, ns – not significant, $^{**}p < 0.01$, $^{***}p < 0.001$, CN ($\times 10^5$) 1.75 versus 7, Student's *t*-test). (**C**) Survival (cells alive after 24 h treatment) was determined by the trypan blue-exclusion method (data are means ± SD; $n = 6$, $^{*}p < 0.05$, $^{**}p < 0.01$, CN ($\times 10^5$) 1.75 versus 7, Student's *t*-test). (D, E) DNA damages were determined using the comet assay after 5 min treatment. One of three independent experiments with comparable outcome is shown (data boxplots of % tail DNA from three tubes/experimental point; $n = 150$, $^{**}p < 0.01$, CN 3.5×10^5 versus 7×10^5, Mann–Whitney *U* test).

H_2O_2 concentrations exerted significantly increased cytotoxicity in the samples with reduced cell number as compared to the reference setting (Fig. 1). Mitochondrial membrane depolarisation as determined after 4 h treatment was significantly increased (Fig. 1A) and proliferation as well as cell survival were significantly reduced as determined by trypan blue after 24 h treatment (Fig. 1B and C). Significantly differing survival data were also achieved after performing the MTT-assay (EZ4U kit, Biomedica, Austria) and ^{3}H-thymidine incorporation (not shown). The screen for apoptosis induction by performing in parallel Annexin V FITC/PI staining (after 4 h treatment) and Hoechst 33258 staining of cytospin preparations (after 4 h and 24 h treatment) demonstrated that HaCat cells undergo negligible apoptotic cell death in response to EGCG and H_2O_2 (not shown). The increased sensitivity of cell number-reduced samples also concerned the induction of DNA damage as analysed by comet assay after 5 min treatment when cell death induction could be ignored (Fig. 1D and E).

3.2. Change of cell number and/or working volume alters extracellular H_2O_2 clearance and cellular oxidative stress

EGCG in aqueous solvent generates H_2O_2 at levels depending on the initial EGCG concentration and time after dissolution. H_2O_2 levels (determined by FOX assay) finally reach plateau values at about the range of the applied EGCG concentrations (not shown). H_2O_2 either generated by EGCG autooxidation or applied directly was rapidly degraded in the presence of HaCat cells. Under reference conditions (7×10^5 cells/2 ml/well), 100 μM H_2O_2 in the cell supernatant had declined to zero 60 min after treatment (Fig. 2A, black squares). In contrast, after application of 100 μM EGCG (generating about 80 μM H_2O_2 within 60 min at cell-free conditions, data not shown) 120 min were needed for complete H_2O_2 degradation (Fig. 2B, black squares). Changes of the experimental settings by both reduction of cell number (at fixed working volume) and vice versa by increasing the working volume (at fixed cell number) significantly reduced the efficacy of H_2O_2 clearance and consequently extended H_2O_2 exposure time of the cells. Thus either a 4-fold increase in working volume or a reduction of cell number to 25%, gave comparable results (Fig. 2A and B, black triangle and open square) and resulted in less effective H_2O_2 clearance (Fig. 2A and B, open triangle). Reduced H_2O_2 clearance was also reflected by a significant increase of the overall cellular oxidative stress (DCFH-DA assay) after H_2O_2 (Fig. 2C) as well as EGCG treatment (Fig. 2D). Control samples were only marginally differing (Fig. 2C).

3.3. Derivation of an algorithm to calculate equally effective EGCG/H_2O_2 concentrations under different experimental conditions

Data shown above provide evidence for a significant impact of the ratio between cell number and working volume on the activity of a given H_2O_2 concentration and consequently also of compounds like EGCG generating ROS upon dissolution. Different assay formats frequently require different cell number/working volume conditions and thus comparison of the derived results is problematic. First we hypothesised that the factor "dose per cell" might be the factor directly determining the cyto- and genotoxic activities of H_2O_2/EGCG as also described by Spitz et al. for the cytotoxicity of H_2O_2 against hamster ovary fibroblasts (Spitz et al., 1987). However, application of this approach failed to predict the exact activity of both EGCG and H_2O_2 in our HACAT cell model under different experimental conditions (data not shown). This might be based on the fact that cells are exposed to a continuously decreasing extracellular amount of H_2O_2 (compare Fig. 1A and B) and in parallel activate cellular protection mechanisms (Elbling et al., 2011). Thus, a simple formula was developed setting in relation drug dose per cell and cellular detoxification based on the following considerations. We deal with settings, where H_2O_2 is depleted by cells over time to zero levels. The impact of H_2O_2 on cells depends on the concentration and time of interaction. Now, when imagining a plot of the concentration of H_2O_2 over-time: concentration decreases from a start value of C, and – after a time of T_{exp} (time of exposure) – the concentration value is practically down to zero. The overall impact of H_2O_2 on cells is determined by the area between this plot and the time axis. Regardless of the exact shape of the H_2O_2 depletion curve (linear or not linear) this area is proportional to the product of C and T_{exp}. Next, we have to consider the time T_{exp}. How long will it take, until H_2O_2 concentration is down to zero? This time does on one hand depend on the total amount of H_2O_2 in the well given by the product of C (in μM) and the working volume (in ml). On the other hand this time will be inversely proportional to the number of cells (CN), based on the observation that a large number of cells deplete H_2O_2 faster than a small number. Thus T_{exp} is proportional to ($C \times V$/CN) (compare Fig. 2A and B). Since we assumed that the impact of H_2O_2 on cells is proportional to $C \times T_{exp}$, we finally reach a proportionality to $C \times (C \times V/\mathrm{CN}) = C^2 \times V/\mathrm{CN}$, which was defined as "cell number volume index (CVI)". With regard to practical applications and use of familiar units a multiplier of 10^3 was included:

$$\mathrm{CVI} = C \ \ (\text{in} \ \ \mu\mathrm{M})^2 \times V \ \ (\text{in} \ \ \mathrm{ml}) \times 10^3/\mathrm{CN} \tag{1A}$$

Each experimental setting is characterized by a defined CVI and we hypothesise that two settings will give comparable results if the CVIs are identical. For settings with different CVIs, concentrations exerting comparable toxicity can easily be deduced by rearrangement of Eq. (1A):

$$C \ \ (\text{in} \ \ \mu\mathrm{M}) = \text{square root}\left(\frac{\mathrm{CVI} \times \mathrm{CN}}{V \times 10^3}\right) \tag{1B}$$

In the following chapters we describe the experimental verification of this algorithm at strongly differing experimental conditions and regarding cyto- and genotoxicity (Figs. 3 and 4) as well as H_2O_2-mediated signal transduction (Fig. 5). Interestingly, correction of the applied concentrations following this algorithm also led to comparable clearance dynamics of EGCG-generated H_2O_2 from the cell culture supernatants (Fig. 4A). This indicates that cyto- and genotoxic effects of EGCG at least in the HaCat cell model predominantly depend on the integrated value of H_2O_2 generation than on peak concentrations.

3.4. Experimental verification of the algorithm: clearance of EGCG-derived H_2O_2 from cell supernatant

Following the formula, equally effective EGCG concentrations were calculated for the three CN settings already used in Figs. 1 and 2 (reference setting compared to 50% and 75% reduced cell number). Cells were treated with EGCG and residual H_2O_2 levels were measured (FOX-assay) at the indicated times with and without algorithm-based correction of EGCG doses (closed and open symbols, respectively, in Fig. 3A). As already demonstrated in Fig. 2B, clearance of H_2O_2 was significantly delayed in the CN reduced settings (reflected by different CVIs as indicated in Fig. 3A). Algorithm-based correction resulted in almost identical H_2O_2 elimination curves in all settings.

3.5. Experimental verification of the algorithm: cytotoxicity and genotoxicity assays

At the identical setting used for the H_2O_2 clearance experiment (Fig. 3A), cell survival was analysed by trypan blue assay. Again, the three different settings resulted in significantly different percentages of cell survival under uncorrected conditions (Fig. 3B, compare Fig. 1B). Algorithm-based concentration adjustment for the reference settings (Fig. 3B) or vice versa for the reduced cell number conditions (Fig. 3C) resulted in comparable cell survival in all cases. The accuracy of calculations was also verified by performing the trypan blue assay with the reference setting in 6-well plates (2 ml working volume) as compared to 96-well plates (200 μl). This corresponds to an increased relative working volume in the 96-well plate as in that setting 70 μl would correspond to the 2 ml situation in the 6-well plate (not shown). Similar results were obtained after performing H_2O_2 instead of EGCG treatment (not shown).

The validity of algorithm-based concentration correction regarding induction of DNA damages (comet assays) by H_2O_2 treatment is shown for the cell number reduced to 25% as compared to the reference setting. Corresponding to computation, identical results were obtained at pairs of different cell numbers and concentrations matching the same CVIs (Fig. 3D and E). Similar CN

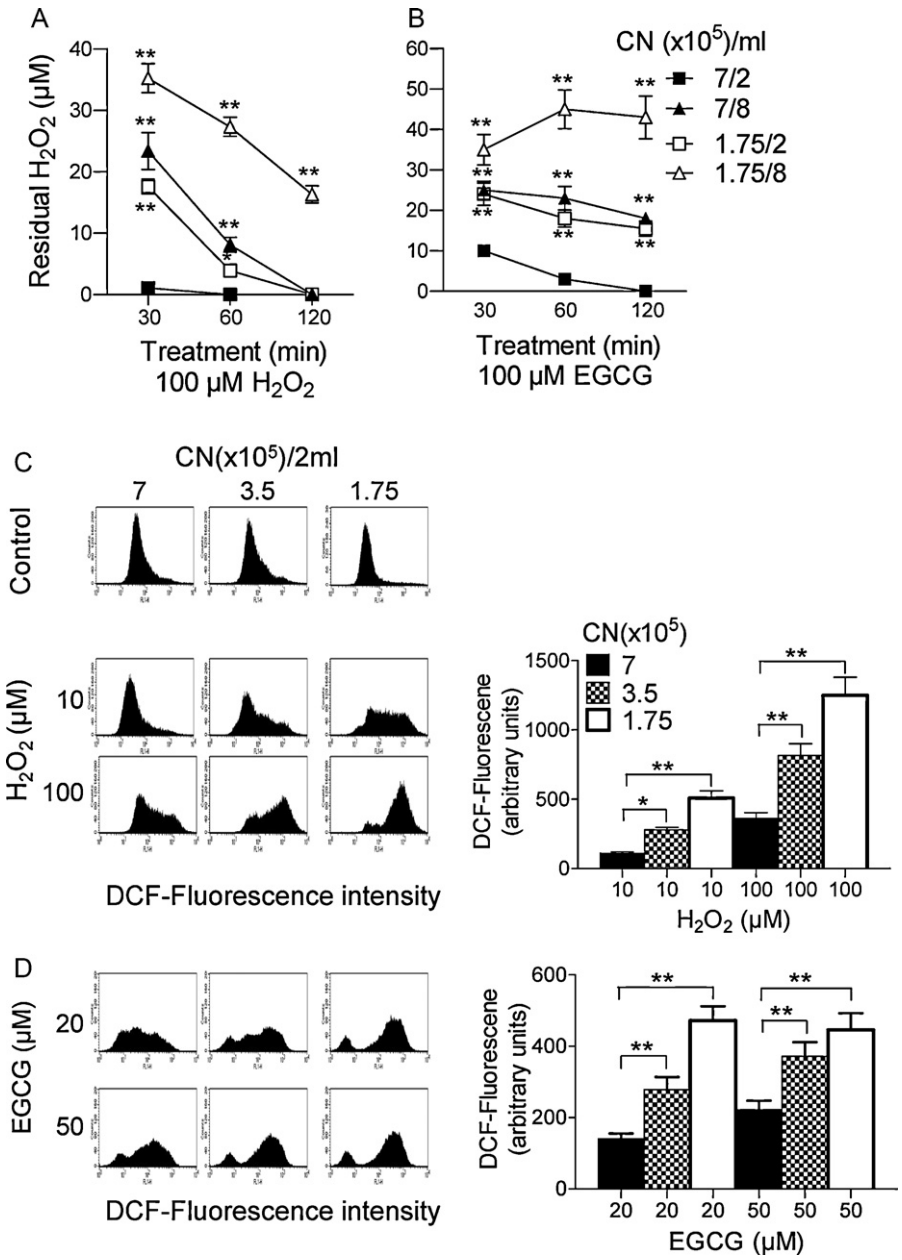

Fig. 2. Changes in cell number/working volume settings affect extracellular H_2O_2 clearance and intracellular ROS generation after EGCG and H_2O_2 treatment. (A, B) Levels of H_2O_2 were measured by FOX assay at the indicated times. CNs ($\times 10^5$)/working volumes (ml) were changed as indicated (data are means ± SD; $n = 6$, $^*p < 0.05$, $^{**}p < 0.01$, versus CN 7×10^5/2 ml, Anova Dunnett's test). (C, D) Intracellular ROS generation was measured by flow cytometry analysis of DCFH-DA stained cells after 1 h treatment. CNs ($\times 10^5$) were changed as indicated and the working volumes were maintained at 2 ml. Representative FACS diagrams of FL-1 (DCF-fluorescence) versus total counts and quantitative analysis of DCF-fluorescence are presented (data are means ± SD; $n = 6$, $^*p < 0.05$, $^{**}p < 0.01$, CN ($\times 10^5$) 3.5 and 1.75 versus 7, Anova Dunnett's test).

dependence was obtained performing EGCG instead of H_2O_2 treatment (not shown).

3.6. Experimental verification of the algorithm: trypan-blue versus clonogenic assay as example for strongly differing assay conditions

Identical EGCG concentrations (10–1000 μM) were analysed by trypan blue staining after 24 h treatment using the reference setting (Fig. 4A and B) compared to the clonogenic survival assay requiring substantially reduced cell number/working volume ratios (Fig. 4C and D). Using identical concentrations without concentration correction, different percentages of cell survival were detected (IC_{50} values of 218.4 μM and 26.9 μM in Fig. 4B and C, respectively). While EGCG at 10 μM was non-toxic (Fig. 4A) but rather growth-stimulating in the trypan blue assay (Fig. 4B) it exerted strong cytotoxicity (50% cell survival) in the CN-reduced clonogenic assay (Fig. 4C). The large divergence of data is also reflected by CVI values calculated for example at 10 μM as 0.285 and 200, respectively. Application of algorithm-based concentration correction in the clonogenic survival assay (all concentrations in Fig. 4D are the algorithm-corrected concentrations of Fig. 4B) led to a cytotoxicity curve perfectly matching between the two conditions. When applying the algorithm in the opposite direction, the measured IC_{50} of 26.9 μM in the clonogenic assay (Fig. 4D, lower panel) corresponded to a computed concentration of 211.1 μM under reference conditions, well comparable to the measured IC_{50} value of 218.4 μM in the trypan blue assay (Fig. 4B). Noticeable, 0.38 μM EGCG in the clonogenic setting (Fig. 4D) indeed matched the growth stimulating effect of the cor-

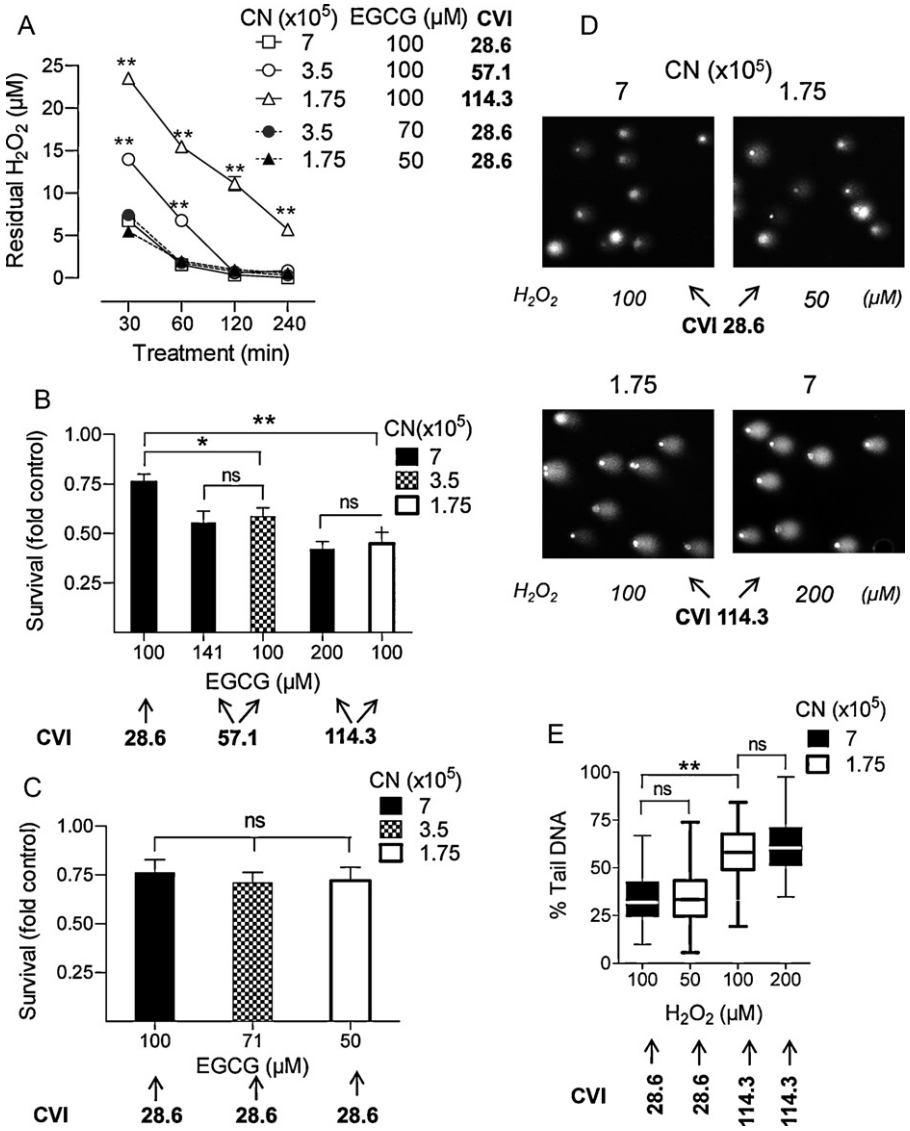

Fig. 3. Experimental verification of the algorithm: clearance of EGCG-derived H_2O_2 from the supernatant, cytotoxicity and genotoxicity. CNs ($\times 10^5$) were used as indicated and all working volumes were maintained at 2 ml. The respective CVI values are indicated in all cases. (A) H_2O_2 levels in the cell supernatant were determined at different time intervals after treatment at constant 100 μM (open symbols) and algorithm-corrected (closed symbols) EGCG concentrations (data are means ± SD; $n = 6$, $^{**}p < 0.01$, versus CN of 7×10^5, Anova Dunnett's test). (B, C) Cell survival analysis as determined by trypan blue method after 24 h EGCG treatment. (B) Treatment of all CNs with 100 μM EGCG and of the reference CN with the algorithm-corrected EGCG concentrations matching the effect under the CN-reduced conditions (data are means ± SD; $n = 6$, $^{*}p < 0.05$, $^{**}p < 0.01$, CN ($\times 10^5$) 7 versus 3.5 and 1.75 and ns – not significant, 3.5 and 1.75 versus 7, Anova Dunnett's test). (C) Algorithm-corrected EGCG concentrations were used in the CN-reduced settings to match the cytotoxicity of 100 μM EGCG at the reference setting (data are means ± SD; $n = 6$, ns – not significant, CN ($\times 10^5$) 3.5 and 1.75 versus 7, Anova Dunnett's test). (D, E) Comet assay was performed after 5 min treatment with H_2O_2. Applied concentrations were adapted following the algorithm as described under (B) and (C). (E) Quantitative analysis of comet assay. One of three independent experiments with comparable outcome is shown (data boxplots of % tail DNA from three tubes/experimental point; $n = 150$, ns – not significant, CN ($\times 10^5$) 7 versus 1.75 and 1.75 versus 7, $^{**}p < 0.01$, CN ($\times 10^5$) 1.75 versus 7, Anova Dunnett's test).

responding 10 μM in the trypan blue assay at reference settings (Fig. 4B).

3.7. Experimental verification of the algorithm: activation of cell signalling

Phosphorylation of the stress-activated protein kinases ERK1/2 after H_2O_2 treatment was analysed under different experimental conditions. At the reference settings, ERK1/2 activation by phosphorylation occurred concentration- and time-dependently with a shift of peak activation from 500 μM at 10 min to 200 μM at 60 min exposure time (Fig. 5A–C). Based on the algorithm, a concentration of 50 μM H_2O_2 at 1.75×10^5 cells/8 ml was calculated to match the effect of 200 μM under the reference settings. Indeed, we observed identical dynamics of ERK1/2 activation (Fig. 5D as compared to Fig. 5A and B). An additional example for the validity of the algorithm is given by computing a setting of 4.5×10^5 cells/8 ml and of 200 μM to induce the same effect (Fig. 5E) as 500 μM under reference conditions (Fig. 5C) with CVI values of 711.1 and 714.3, respectively. Together these data prove even in the sensitive issue of signal transduction activation the validity of the algorithm.

4. Discussion

One common feature shared by several polyphenolic compounds is their sensitivity to autooxidation *in vitro* (Halliwell, 2008; Lambert et al., 2007b; Long et al., 2007, 2010; Sang et al., 2007). EGCG undergoes oxidative polymerization with concomitant H_2O_2 production (Hong et al., 2002; Long et al., 2000) depending on culture media as well as differences in the potency of media to catalyse

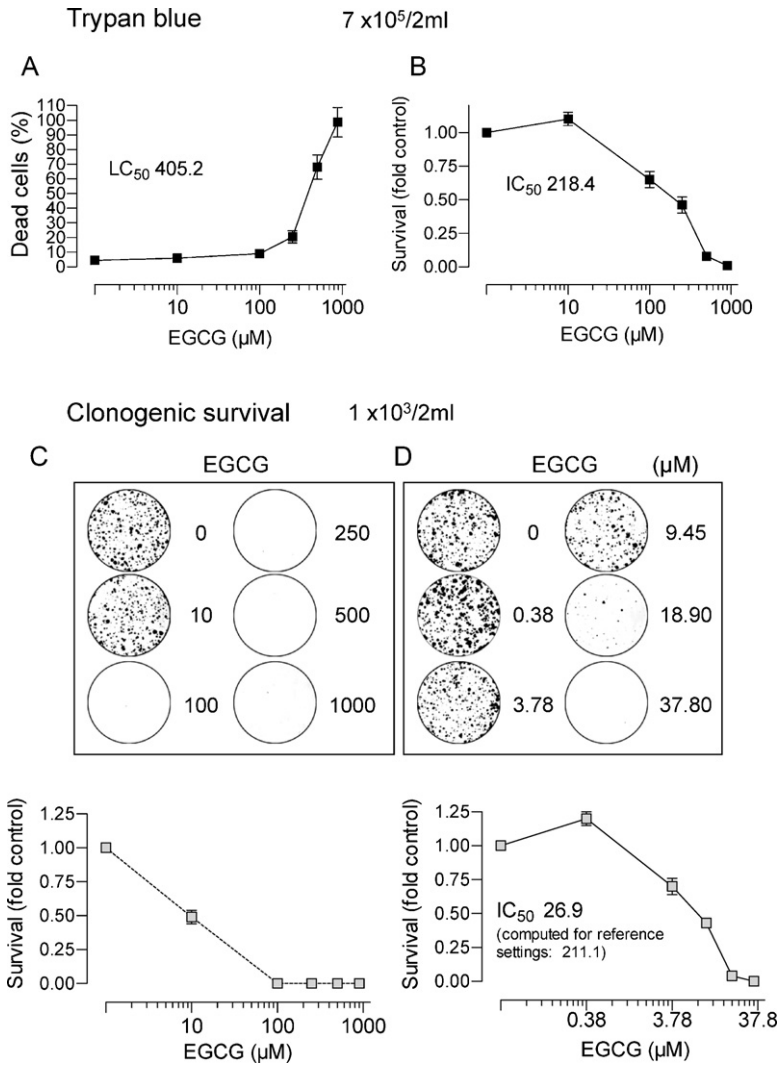

Fig. 4. Experimental verification of the algorithm: survival/proliferation assays. (A, B) Cell death (A) and cell survival (B) were determined by the trypan blue method after 24 h EGCG treatment and under the reference setting condition as indicated. (C, D) Clonogenic survival 10 d after EGCG treatment and the reference setting condition as indicated was determined by crystal violet staining. Representative photographs of stained wells (upper panels) are opposed to the quantitative evaluations (lower panels) by reading crystal violet extinction (OD_{595} nm) after dye solution with Sorenson's buffer (means ± SD; $n = 6$). (C) Clonogenic assays with the identical EGCG concentrations used for reference setting in A and B. (D) Clonogenic assays with EGCG concentrations algorithm-corrected for those used under reference settings in (B).

the generated H_2O_2 (Long and Halliwell, 2009). Cytotoxic and genotoxic effects (Long et al., 2007) as well as biological effects (Hou et al., 2005; Lambert and Elias, 2010) have been associated with the extent and rate of H_2O_2 production (Elbling et al., 2005; Halliwell, 2008; Lambert and Elias, 2010; Long and Halliwell, 2009; Long et al., 2007; Yang et al., 2000) based on the almost complete reversion by presence of antioxidant enzymes in the reaction medium (Elbling et al., 2005; Hou et al., 2005; Li et al., 2010; Yang et al., 2000). Considering the detrimental effects of high EGCG concentrations, it has recurrently been questioned whether autooxidation may also occur *in vivo* (Halliwell, 2008). Toxic effects of EGCG observed *in vivo* following consumption of dietary supplements in humans (Mazzanti et al., 2009) and administration of tea extracts in animal studies (Lambert et al., 2010) were considered as based on prooxidant activities of EGCG (Lambert et al., 2010). A recent study gave striking evidence for *in vivo* ROS formation in human lung cancer xenograft tissues after EGCG treatment in mice (Li et al., 2010). In addition, we recently demonstrated that autooxidation-derived H_2O_2 is significantly involved in EGCG-mediated protection against H_2O_2-induced cell damage *in vitro* (Elbling et al., 2011). In view of these data the prooxidant potency should be included in the analysis of the impact of EGCG at toxic and non-toxic concentrations.

In this study we demonstrate that under subconfluent culture conditions changes of the cell number/working volume ratio result in pronounced differences in the cytotoxic, DNA-damaging and signal transducing effectiveness of prooxidant EGCG as compared to pure H_2O_2 in HaCat keratinocytes. This leads to the surprising observation that e.g. EGCG at 10 μM can induce either enhanced cell proliferation or distinct cytotoxicity depending on the experimental setting.

Cell density dependency as previously shown for the cytotoxicity of H_2O_2 by means of mouse (Long et al., 2003) and Chinese hamster ovary fibroblast (Spitz et al., 1987), HeLa cells (Bello et al., 2003) and also the immortalized HaCat keratinocytes (Bakondi et al., 2003) was attributed to confluence-dependent mechanisms including the inhibition of poly(ADP-ribose) polymerase and caspase-mediated apoptotic pathways (Bakondi et al., 2003; Long et al., 2003) and increased expression of the cellular antioxidants regenerating (Shirabe et al., 1995) NADH–cytochrome b_5 reductase (Bello et al., 2003; Bello et al., 2001). Confluence-elicited growth arrest shows distinct alterations in transcriptional

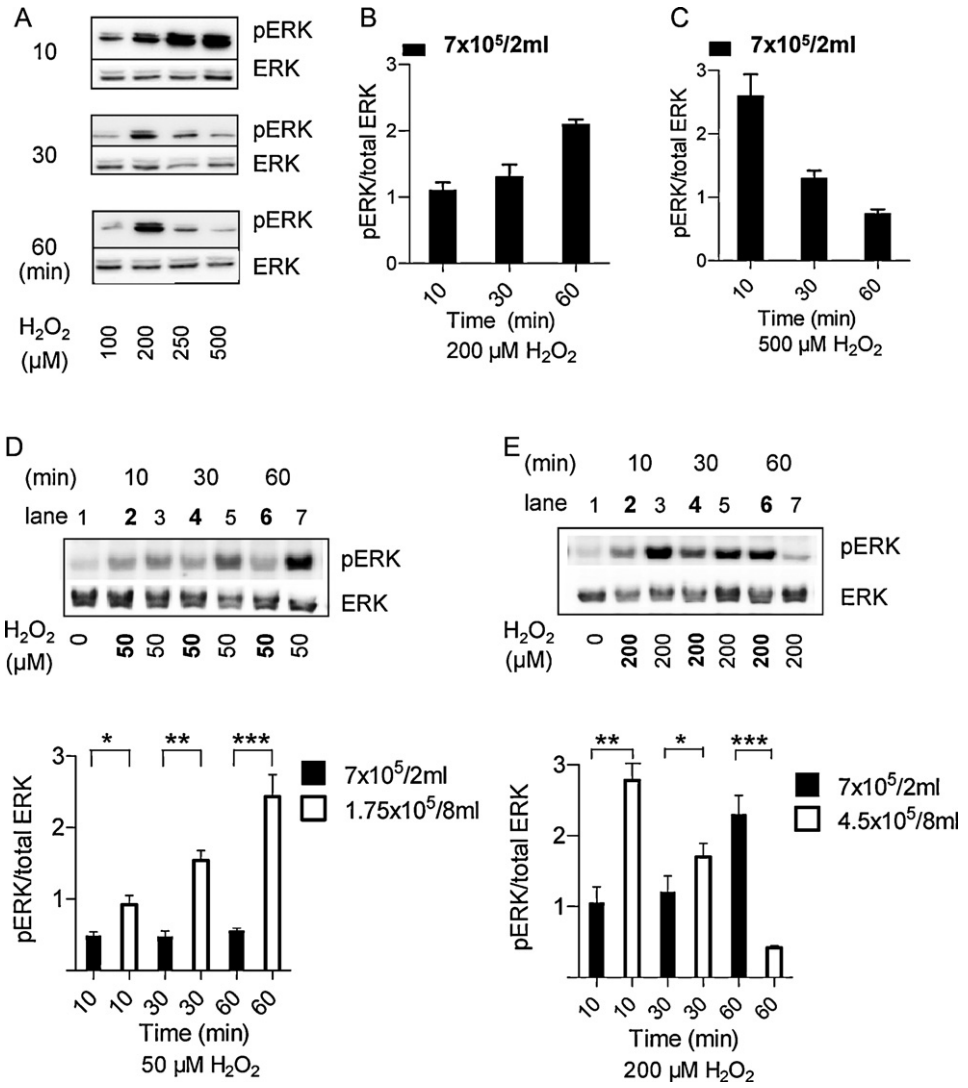

Fig. 5. Experimental verification of the algorithm: activation of cell signalling. Total cell extracts were prepared at different times of H_2O_2 treatment (concentrations as indicated) and probed for phospho-(p)ERK1/2 and total ERK1/2. (A) Representative blots from treatment experiments using reference setting as indicated and (B, C) optical density measurements of the respective pERK/total ERK ratios (mean ± SD; $n = 3$) for 200 and 500 μM, respectively. Mean of three independent experiments. (D, E) Representative blots (upper panels) and quantitative evaluations (lower panels) derived from H_2O_2 treatment experiments under reference setting conditions (lanes 2, 4, 6 in bold type and black columns) as compared to algorithm-calculated settings matching results obtained with the reference setting. (D) Alternative setting of 1.75×10^5/8 ml and (E) 4.5×10^5/8 ml (lanes 3, 5, 7 and white columns) (data are means ± SD; $n = 3$, $^*p < 0.05$, $^{**}p < 0.01$, $^{***}p < 0.001$, alternative versus reference setting, Student's *t*-test).

activation (Kaluz et al., 2002; Sheta et al., 2001), decreased intracellular ROS levels (Pani et al., 2000) as well as modified expression patterns of growth factors (Koura et al., 1996; Mukhopadhyay et al., 1998; Sun et al., 1994) and antioxidant systems (Bello et al., 2003, 2001; Bravard et al., 1999; Phillips et al., 1994). In contrast to the above-mentioned studies on H_2O_2 density dependence we used HaCat keratinocytes at subconfluent conditions to exclude the special properties of cells in lag phase due to contact inhibition.

Consistent with the observed impact of experimental settings regarding cell number per working volume on EGCG activities, other ROS generating compounds have been reported to be susceptible to cell density conditions. Thus cell density dependence has been reported for the polyphenolic isoflavonoid Pterocarpans (Maurich et al., 2006), further cannabidiol (Ramer et al., 2009) generating NAD(P)H oxidase-mediated ROS (McKallip et al., 2006) and ascorbic acid (Preobrazhensky et al., 2001) autooxidizing (superoxide anion) upon solubilisation (Long and Halliwell, 2009). In our study, the pronounced effect of altered cell number/working volume ratios was proven to be based on altered clearance of autooxidation-derived H_2O_2 and pure H_2O_2 from the cell supernatant. This is in accordance with the loss of toxicity of the cell supernatant as shown previously for H_2O_2 cell density dependence (Spitz et al., 1987). Alterations of the experimental settings in our proliferating HaCat cell model led to a severe change in the clearance efficacy of H_2O_2 from the cell supernatant. Reduction of the cell number and/or increase of the working volume significantly extended the time to complete H_2O_2 depletion. Consequently, we concluded that prolongation of EGCG/H_2O_2-mediated oxidative stress is responsible for the distinctly altered efficacy in terms of cyto- and genotoxicity.

To address the problem of EGCG/H_2O_2 density dependence, we first set out to correct the data by considering the parameter dose/cell as suggested in one study regarding H_2O_2 cytotoxicity in Chinese hamster ovary fibroblasts (Spitz et al., 1987). Unexpectedly, this parameter did not precisely correct for either EGCG or pure H_2O_2 density dependence in our HaCat cell model. One possible explanation might be the fact that cells are exposed to a continuously decreasing extracellular amount of H_2O_2 based on continuous cell-dependent clearance and in parallel activation of

cellular protection mechanisms by EGCG-derived H_2O_2 in HaCat cells (Elbling et al., 2011).

On the basis of theoretical consideration as outlined in the result chapter and involving the clearance behavior pattern of EGCG-generated H_2O_2 from the cell supernatants, we have deduced and validated a straight forward algorithm setting by relating EGCG/H_2O_2 concentration, working volume, cell number and, although indirectly, the exposure time. By using this algorithm a so-called cell number volume index (CVI) can be calculated for each experimental setting. By means of this CVI, concentrations that are equally effective under different settings can be deduced. The accuracy of algorithm-calculated concentrations was proven not only for cytotoxicity but also for rapid DNA damage and the complex issue of dose- and time-dependent MAP-kinase activation measured by ERK phosphorylation. Particularly to emphasize is the verification of identical H_2O_2 clearance curves after treatment with algorithm-based EGCG concentration under different setting conditions.

5. Concluding remarks

Using proliferating HaCat cells, we show a pronounced cell number/working volume dependence of EGCG-mediated cellular effect based on different clearance kinetics of autooxidation-generated H_2O_2. The EGCG concentrations used in this study were in the range mostly used in experiments with cell lines. EGCG cell number/working volume dependence is not a sole characteristic of HaCat cells and has been observed basically in all cell models we have investigated so far including several malignant cell types (data not shown). This implies that experimental settings have to be considered and strictly controlled when investigating prooxidant effects of EGCG and probably also of other autooxidizing polyphenols *in vitro*. Human keratinocyte-derived cells were applied in these studies based on the consideration that these cells have widely retained their normal phenotype (Boukamp et al., 1988) and keratinocytes represent oral and skin epithelial cells frequently exposed to EGCG/H_2O_2 via green tea consumption, nutritional supplements or cosmetics.

Conflict of interest statement

None declared.

Acknowledgements

This study was funded by the Herzfelder'schen Familienstiftung. We are indebted to Elisabeth Rabensteiner and Marlies Spannberger for technical assistance and Paul Breit for preparing photographs.

References

Afaq, F., Adhami, V.M., Ahmad, N., Mukhtar, H., 2003. Inhibition of ultraviolet B-mediated activation of nuclear factor [kappa]B in normal human epidermal keratinocytes by green tea Constituent (-)-epigallocatechin-3-gallate. Oncogene 22, 1035–1044.

Ahmad, N., Cheng, P., Mukhtar, H., 2000. Cell cycle dysregulation by green tea polyphenol epigallocatechin-3-gallate. Biochem. Biophys. Res. Commun. 275, 328–334.

Anderson, R.F., Fisher, L.J., Hara, Y., Harris, T., Mak, W.B., Melton, L.D., Packer, J.E., 2001. Green tea catechins partially protect DNA from (•)OH radical-induced strand breaks and base damage through fast chemical repair of DNA radicals. Carcinogenesis 22, 1189–1193.

Bakondi, E., Gonczi, M., Szabo, E., Bai, P., Pacher, P., Gergely, P., Kovacs, L., Hunyadi, J., Szabo, C., Csernoch, L., Virag, L., 2003. Role of intracellular calcium mobilization and cell-density-dependent signaling in oxidative-stress-induced cytotoxicity in HaCaT keratinocytes. J. Invest. Dermatol. 121, 88–95.

Bello, R.I., Alcaín, F.J., Gómez-Díaz, C., López-Lluch, G., Navas, P., Villalba, J.M., 2003. Hydrogen peroxide- and cell-density-regulated expression of NADH–cytochrome b5 reductase in HeLa cells. J. Bioenerg. Biomemb. 35, 169–179.

Bello, R.I., Gomez-Diaz, C., Navarro, F., Alcain, F.J., Villalba, J.M., 2001. Expression of NAD(P)H:quinone oxidoreductase 1 in HeLa cells: role of hydrogen peroxide and growth phase. J. Biol. Chem. 276, 44379–44384.

Boukamp, P., Petrussevska, R.T., Breitkreutz, D., Hornung, J., Markham, A., Fusenig, N.E., 1988. Normal keratinization in a spontaneously immortalized aneuploid human keratinocyte cell line. J. Cell Biol. 106, 761–771.

Bravard, A., Petridis, F., Luccioni, C., 1999. Modulation of antioxidant enzymes p21WAF1 and p53 expression during proliferation and differentiation of human melanoma cell lines. Free Radic. Biol. Med. 26, 1027–1033.

Burlinson, B., Tice, R.R., Speit, G., Agurell, E., Brendler-Schwaab, S.Y., Collins, A.R., Escobar, P., Honma, M., Kumaravel, T.S., Nakajima, M., Sasaki, Y.F., Thybaud, V., Uno, Y., Vasquez, M., Hartmann, A., Beevers, C., Brendler-Schwaab, S., Clay, P., Collins, A., Smith, A., Anderson, D., Kobayashi, H., Miyamae, Y., Rojas, E., Ryu, J.C., 2007. Fourth international workgroup on genotoxicity testing: results of the in vivo Comet assay workgroup. Mutat. Res. 627, 31–35.

Collins, A.R., 2004. The comet assay for DNA damage and repair: principles, applications, and limitations. Appl. Biochem. Biotechnol. B: Mol. Biotechnol. 26, 249–261.

Elbling, L., Herbacek, I., Weiss, R.-M., Jantschitsch, C., Micksche, M., Gerner, C., Pangratz, H., Grusch, M., Knasmüller, S., Berger, W., 2011. Hydrogen peroxide mediates EGCG-induced antioxidant protection in human keratinocytes. Free Radic. Biol. Med. 49, 1444–1452.

Elbling, L., Weiss, R.M., Teufelhofer, O., Uhl, M., Knasmueller, S., Schulte-Hermann, R., Berger, W., Micksche, M., 2005. Green tea extract and (−)-epigallocatechin-3-gallate, the major tea catechin, exert oxidant but lack antioxidant activities. FASEB J. 19, 807–809.

Elmets, C.A., Singh, D., Tubesing, K., Matsui, M., Katiyar, S., Mukhtar, H., 2001. Cutaneous photoprotection from ultraviolet injury by green tea polyphenols. J. Am. Acad. Dermatol. 44, 425–432.

Gutteridge, J.M.C., Halliwell, B., 2010. Antioxidants: molecules, medicines, and myths. Biochem. Biophys. Res. Commun. 393, 561–564.

Halliwell, B., 2008. Are polyphenols antioxidants or pro-oxidants? What do we learn from cell culture and in vivo studies? Arch. Biochem. Biophys. 7, 7.

Heffeter, P., Jakupec, M.A., Korner, W., Wild, S., von Keyserlingk, N.G., Elbling, L., Zorbas, H., Korynevska, A., Knasmuller, S., Sutterluty, H., Micksche, M., Keppler, B.K., Berger, W., 2006. Anticancer activity of the lanthanum compound [tris(1,10-phenanthroline)lanthanum(III)]trithiocyanate (KP772; FFC24). Biochem. Pharmacol. 71, 426–440.

Higdon, J.V., Frei, B., 2003. Tea catechins and polyphenols: health effects, metabolism, and antioxidant functions. Crit. Rev. Food Sci. Nutr. 43, 89–143.

Hong, J., Lu, H., Meng, X., Ryu, J.H., Hara, Y., Yang, C.S., 2002. Stability, cellular uptake, biotransformation, and efflux of tea polyphenol (−)-epigallocatechin-3-gallate in HT-29 human colon adenocarcinoma cells. Cancer Res. 62, 7241–7246.

Hou, Z., Lambert, J.D., Chin, K.-V., Yang, C.S., 2004. Effects of tea polyphenols on signal transduction pathways related to cancer chemoprevention. Mutat. Res./Fundam. Mol. Mech. Mutagen. 555, 3–19.

Hou, Z., Sang, S., You, H., Lee, M.J., Hong, J., Chin, K.V., Yang, C.S., 2005. Mechanism of action of (−)-epigallocatechin-3-gallate: auto-oxidation-dependent inactivation of epidermal growth factor receptor and direct effects on growth inhibition in human esophageal cancer KYSE 150 cells. Cancer Res. 65, 8049–8056.

Ikigai, H., Nakae, T., Hara, Y., Shimamura, T., 1993. Bactericidal catechins damage the lipid bilayer. Biochim. Biophys. Acta 1147, 132–136.

Kaluz, S., Kaluzova, M., Chrastina, A., Olive, P.L., Pastorekova, S., Pastorek, J., Lerman, M.I., Stanbridge, E.J., 2002. Lowered oxygen tension induces expression of the hypoxia marker MN/carbonic anhydrase IX in the absence of hypoxia-inducible factor 1{alpha} stabilization: a role for phosphatidylinositol 3′-kinase. Cancer Res. 62, 4469–4477.

Khan, N., Afaq, F., Saleem, M., Ahmad, N., Mukhtar, H., 2006. Targeting multiple signaling pathways by green tea polyphenol (−)-epigallocatechin-3-gallate. Cancer Res. 66, 2500–2505.

Khan, N., Mukhtar, H., 2007. Tea polyphenols for health promotion. Life Sci. 81, 519–533.

Koura, A.N., Liu, W., Kitadai, Y., Singh, R.K., Radinsky, R., Ellis, L.M., 1996. Regulation of vascular endothelial growth factor expression in human colon carcinoma cells by cell density. Cancer Res. 56, 3891–3894.

Lambert, J.D., Elias, R.J., 2010. The antioxidant and pro-oxidant activities of green tea polyphenols: A role in cancer prevention. Arch. Biochem. Biophys. 501, 65–72.

Lambert, J.D., Kennett, M.J., Sang, S., Reuhl, K.R., Ju, J., Yang, C.S., 2010. Hepatotoxicity of high oral dose (−)-epigallocatechin-3-gallate in mice. Food Chem. Toxicol. 48, 409–416.

Lambert, J.D., Sang, S., Yang, C.S., 2007a. Biotransformation of green tea polyphenols and the biological activities of those metabolites. Mol. Pharm. 4, 819–825.

Lambert, J.D., Sang, S., Yang, C.S., 2007b. Possible controversy over dietary polyphenols: benefits vs risks. Chem. Res. Toxicol. 20, 583–585.

Li, G.X., Chen, Y.K., Hou, Z., Xiao, H., Jin, H., Lu, G., Lee, M.J., Liu, B., Guan, F., Yang, Z., Yu, A., Yang, C.S., 2010. Pro-oxidative activities and dose–response relationship of (−)-epigallocatechin-3-gallate in the inhibition of lung cancer cell growth: a comparative study in vivo and in vitro. Carcinogenesis 31, 902–910.

Long, H., Han, H., Yang, B., Wang, Z., 2003. Opposite cell density-dependence between spontaneous and oxidative stress-induced apoptosis in mouse fibroblast L-cells. Cell. Physiol. Biochem. 13, 401–414.

Long, L.H., Clement, M.V., Halliwell, B., 2000. Artifacts in cell culture: rapid generation of hydrogen peroxide on addition of (−)-epigallocatechin, (−)-

epigallocatechin gallate, (+)-catechin, and quercetin to commonly used cell culture media. Biochem. Biophys. Res. Commun. 273, 50–53.
Long, L.H., Halliwell, B., 2009. Artefacts in cell culture: pyruvate as a scavenger of hydrogen peroxide generated by ascorbate or epigallocatechin gallate in cell culture media. Biochem. Biophys. Res. Commun. 388, 700–704.
Long, L.H., Hoi, A., Halliwell, B., 2010. Instability of, and generation of hydrogen peroxide by, phenolic compounds in cell culture media. Arch. Biochem. Biophys. 501, 162–169.
Long, L.H., Kirkland, D., Whitwell, J., Halliwell, B., 2007. Different cytotoxic and clastogenic effects of epigallocatechin gallate in various cell-culture media due to variable rates of its oxidation in the culture medium. Mutat. Res. – Genet. Toxicol. Environ. Mutagen. 634, 177–183.
Maurich, T., Iorio, M., Chimenti, D., Turchi, G., 2006. Erybraedin C and bitucarpin A, two structurally related pterocarpans purified from Bituminaria bituminosa, induced apoptosis in human colon adenocarcinoma cell lines MMR- and p53-proficient and -deficient in a dose-, time-, and structure-dependent fashion. Chem. Biol. Interact. 159, 104–116.
Mazzanti, G., Menniti-Ippolito, F., Moro, P.A., Cassetti, F., Raschetti, R., Santuccio, C., Mastrangelo, S., 2009. Hepatotoxicity from green tea: a review of the literature and two unpublished cases. Eur. J. Clin. Pharmacol. 65, 331–341 (Epub 2009 February 2006).
McKallip, R.J., Jia, W., Schlomer, J., Warren, J.W., Nagarkatti, P.S., Nagarkatti, M., 2006. Cannabidiol-induced apoptosis in human leukemia cells: a novel role of cannabidiol in the regulation of p22phox and Nox4 expression. Mol. Pharmacol. 70, 897–908.
Mukhopadhyay, D., Tsiokas, L., Sukhatme, V.P., 1998. High cell density induces vascular endothelial growth factor expression via protein tyrosine phosphorylation. Gene Exp. 7, 53–60.
Na, H.K., Kim, E.H., Jung, J.H., Lee, H.H., Hyun, J.W., Surh, Y.J., 2008. (−)-Epigallocatechin gallate induces Nrf2-mediated antioxidant enzyme expression via activation of PI3K and ERK in human mammary epithelial cells. Arch. Biochem. Biophys. 476, 171–177, Epub 2008 Apr 2006.
Nguyen, T., Nioi, P., Pickett, C.B., 2009. The Nrf2-antioxidant response element signaling pathway and its activation by oxidative stress. J. Biol. Chem. 284, 13291–13295 (Epub 12009 January 13230).
Pani, G., Colavitti, R., Bedogni, B., Anzevino, R., Borrello, S., Galeotti, T., 2000. A redox signaling mechanism for density-dependent inhibition of cell growth. J. Biol. Chem. 275, 38891–38899.
Phillips, R.M., de la Cruz, A., Traver, R.D., Gibson, N.W., 1994. Increased activity and expression of NAD(P)H:quinone acceptor oxidoreductase in confluent cell cultures and within multicellular spheroids. Cancer Res. 54, 3766–3771.
Preobrazhensky, S., Malugin, A., Wentz, M., 2001. Flow cytometric assay for evaluation of the effects of cell density on cytotoxicity and induction of apoptosis. Cytometry 43, 199–203.
Ramer, R., Merkord, J., Rohde, H., Hinz, B., 2009. Cannabidiol inhibits cancer cell invasion via upregulation of tissue inhibitor of matrix metalloproteinases-1. Biochem. Pharmacol. 79, 955–966.
Royall, J.A., Ischiropoulos, H., 1993. Evaluation of 2′,7′-dichlorofluorescin and dihydrorhodamine 123 as fluorescent probes for intracellular H_2O_2 in cultured endothelial cells. Arch. Biochem. Biophys. 302, 348–355.
Sang, S., Hou, Z., Lambert, J.D., Yang, C.S., 2005. Redox properties of tea polyphenols and related biological activities. Antioxid. Redox Signal. 7, 1704–1714.
Sang, S., Yang, I., Buckley, B., Ho, C.T., Yang, C.S., 2007. Autoxidative quinone formation in vitro and metabolite formation in vivo from tea polyphenol (−)-epigallocatechin-3-gallate: studied by real-time mass spectrometry combined with tandem mass ion mapping. Free Radic. Biol. Med. 43, 362–371.
Sheta, E.A., Trout, H., Gildea, J.J., Harding, M.A., Theodorescu, D., 2001. Cell density mediated pericellular hypoxia leads to induction of HIF-1alpha via nitric oxide and Ras/MAP kinase mediated signaling pathways. Oncogene 20, 7624–7634.
Shirabe, K., Landi, M.T., Takeshita, M., Uziel, G., Fedrizzi, E., Borgese, N., 1995. A novel point mutation in a 3′ splice site of the NADH-cytochrome b5 reductase gene results in immunologically undetectable enzyme and impaired NADH-dependent ascorbate regeneration in cultured fibroblasts of a patient with type II hereditary methemoglobinemia. Am. J. Hum. Genet. 57, 302–310.
Song, J.-M., Lee, K.-H., Seong, B.-L., 2005. Antiviral effect of catechins in green tea on influenza virus. Antivir. Res. 68, 66–74.
Spitz, D.R., Dewey, W.C., Li, G.C., 1987. Hydrogen peroxide or heat shock induces resistance to hydrogen peroxide in Chinese hamster fibroblasts. J. Cell. Physiol. 131, 364–373.
Sun, L., Wu, S., Coleman, K., Fields, K.C., Humphrey, L.E., Brattain, M.G., 1994. Autocrine transforming growth factor-beta 1 and beta 2 expression is increased by cell crowding and quiescence in colon carcinoma cells. Exp. Cell Res. 214, 215–224.
Tice, R.R., Agurell, E., Anderson, D., Burlinson, B., Hartmann, A., Kobayashi, H., Miyamae, Y., Rojas, E., Ryu, J.C., Sasaki, Y.F., 2000. Single cell gel/comet assay: guidelines for in vitro and in vivo genetic toxicology testing. Environ. Mol. Mutagen. 35, 206–221.
Wang, H., Joseph, J.A., 1999. Quantifying cellular oxidative stress by dichlorofluorescein assay using microplate reader. Free Radic. Biol. Med. 27, 612–616.
Wolff, S.P., 1994. [18]Ferrous ion oxidation in presence of ferric ion indicator xylenol orange for measurement of hydroperoxides. Methods in enzymology. In: Packer, L. (Ed.), Oxygen Radicals in Biological Systems Part C. Academic Press, pp. 182–189.
Yang, C.S., Lambert, J.D., Hou, Z., Ju, J., Lu, G., Hao, X., 2006. Molecular targets for the cancer preventive activity of tea polyphenols. Mol. Carcinog. 45, 431–435.
Yang, C.S., Lambert, J.D., Ju, J., Lu, G., Sang, S., 2007. Tea and cancer prevention: molecular mechanisms and human relevance. Toxicol. Appl. Pharmacol. 224, 265–273.
Yang, C.S., Lambert, J.D., Sang, S., 2009a. Antioxidative and anti-carcinogenic activities of tea polyphenols. Arch. Toxicol. 83, 11–21.
Yang, C.S., Maliakal, P., Meng, X., 2002. Inhibition of carcinogenesis by tea. Annu. Rev. Pharmacol. Toxicol. 42, 25–54.
Yang, C.S., Wang, X., Lu, G., Picinich, S.C., 2009b. Cancer prevention by tea: animal studies, molecular mechanisms and human relevance. Nat. Rev. Cancer 9, 429–439.
Yang, G.Y., Liao, J., Li, C., Chung, J., Yurkow, E.J., Ho, C.T., Yang, C.S., 2000. Effect of black and green tea polyphenols on c-jun phosphorylation and H(2)O(2) production in transformed and non-transformed human bronchial cell lines: possible mechanisms of cell growth inhibition and apoptosis induction. Carcinogenesis 21, 2035–2039.
Yu, R., Chen, C., Mo, Y.Y., Hebbar, V., Owuor, E.D., Tan, T.H., Kong, A.N., 2000. Activation of mitogen-activated protein kinase pathways induces antioxidant response element-mediated gene expression via a Nrf2-dependent mechanism. J. Biol. Chem. 275, 39907–39913.